## Current Limitation and Speed Drop Minimization in Optimal-Efficiency of Induction Motors

M. Ebrahimi<sup>1</sup> M. Moallem<sup>2</sup> M.H. Ershadi<sup>3</sup> A.H. Ebrahimi<sup>4</sup>

#### Abstract:

In conventional direct torque control (DTC), the stator flux is usually kept constant by controlling the x-axis component of the stator voltage in the stator flux reference frame. The torque is then controlled by the y-axis component of stator voltage. In this scenario, the stator current does not exceed its permissible value. However, in the so-called optimal efficiency mode, the induction motor operates with reduced flux-level at light loads. The reference flux increases with the increase in the load torque. Consequently, stator current overshoots from its threshold, and the inverter's rated power needs to be increased. When the load torque increases suddenly, speed will drop significantly as the flux level had been initially reduced. In this paper, the origin of this phenomenon and the overshoot current are described using the equivalent circuit model of an induction motor. A current limiting strategy is then proposed for the DTC drive with a torque controller. Also to improve dynamic response, an algorithm for optimum distribution of stator current is developed that includes flux and torque components. This algorithm produces the maximum feasible output torque and minimizes the speed drop. Numerical simulation verifies the efficiency and efficacy of both proposed methodologies.

**Keywords:** Current Limitation, Direct Torque Control, Induction Motor, Optimal Efficiency, Speed Drop Minimization.

Submission date: 25, Jan., 2014

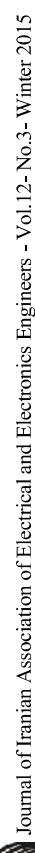
Conditionally Acceptance date: 4, Oct., 2014

Acceptance date: 2, July, 2015

Corresponding author: M.Ebrahimi

Corresponding author's address: Department of Electrical and Computer Engineering, Isfahan University of

Technology, Isfahan, Iran.



<sup>&</sup>lt;sup>1</sup> Assoc. Prof., Department of Electrical and Computer Engineering, Isfahan University of Technology, Isfahan, Iran mebrahim@cc.iut.ac.ir

<sup>&</sup>lt;sup>2</sup> Prof., Department of Electrical and Computer Engineering, Isfahan University of Technology, Isfahan, Iran <a href="moallem@cc.iut.ac.ir">moallem@cc.iut.ac.ir</a>

<sup>&</sup>lt;sup>3</sup> Ph.D. Student, Department of Electrical and Computer Engineering, Isfahan University of Technology, Isfahan, Iran <a href="mailto:ershadi@ec.iut.ac.ir">ershadi@ec.iut.ac.ir</a>

<sup>&</sup>lt;sup>4</sup> Student, Department of Electrical and Computer Engineering, Isfahan University of Technology, Isfahan, Iran amirhosein.ebrahimi93@gmail.com

Journal of Iranian Association of Electrical and Electronics Engineers - Vol.12- No.3- Winter 2015

### 1. Introduction

Direct torque control (DTC) of induction machines allows a decoupled control of flux and torque, and provides fast and robust operation of the drive [1-3, 28]. Classical DTC decouples the control of flux and torque using hysteresis control of flux, torque error, and flux position. A switching look up table selects voltage vectors feeding the induction motor. To address the drawbacks of classical DTC, a voltage modulation scheme replaces the look-up table for the purpose of voltage vector selection [4]. The modulation scheme is essentially based on the well-known space-vector modulation (SVM) with a constant switching frequency [5].

PI controllers can replace hysteresis controllers to generate the direct and quadrature components of voltage from stator flux and torque errors, respectively [6]. This leads to good transient performance, robustness and reduced torque ripple. In recent years, DTC-SVM is applied to multilevel inverters for higher power applications [7], [8].

Another important objective in induction motor drive is to achieve maximum efficiency. Numerous operation schemes have been proposed for the optimal choice of the flux level for a given load [9,10, 29]. These techniques can be divided into two categories. The first category is the loss model-based approach [11]- [13], which computes losses by using the machine model, and selects a flux level that minimizes the losses. The second category is the search controller technique [9], [14], [15], in which, the flux is decreased until the input power settles at the lowest value for the given torque and speed. Regardless of the loss minimizing technique employed, the induction motor will always operates with reduced flux level at light loads [16], [17].

A particular challenge in DTC-SVM drives with a torque controller would be to limit the stator current in case of a sudden load change and avoid current overshoot and subsequent overdesign of the inverter. Thus, it is highly desired to study the current overshoot phenomena and propose a suitable current limiting strategy. As well as in DTC-SVM drive with a speed controller, the challenge is to achieve the minimum time response or drop in speed if a sudden increase in load happens.

Furthermore, the maximum available stator current is limited by the inverter rating. Therefore, the problem reduces to determination of the optimal subdivision of the available maximum stator current into the flux producing and torque producing current components, such that the maximum dynamic torque is produced while, at the same time, the rated flux is re-established. Optimum efficiency controller is normally disabled during such transients and the current subdivision components are determined according to a certain algorithm.

The simplest approach, that preserves decoupling the flux and torque production, is to retain the existing value of the flux-producing current component, and use the remaining inverter current capability to maximize torque [18]. This method is, however, characterized with very slow transient response. In an alternative method, it is recommended first to use all of the available current to produce flux, such that the change in torque is initially zero. Once the flux is built up, all of the available inverter current is channeled into the torque-producing current component [19]. This strategy can support much higher transient torques.

An optimal dynamic stator current distribution is presented in [20]. The criterion used is to minimize the speed drop due to the sudden increase in load torque. This strategy improves the torque response, but the stator current components are functions of the load torque. Another control scheme for robust fluxweakening operation of DTC drive is proposed in [21]. The basic idea is to adjust the flux reference on the basis of the torque error. In this method, it is necessary to estimate the maximum torque that the induction machine can generate at any speed. A dynamic overmodulation strategy for fast dynamic torque control in DTC-hysteresis-based drive is proposed in [22]. To achieve the fastest dynamic torque response, the voltage vector that produces the largest tangential component to the circular flux locus has been used. Alternatively, this paper strives to achieve the fastest dynamic

Torque response and to minimize the speed drop.

The paper is organized as follows. The principles of DTC-SVM is described in section 2. Using the static and dynamic models of induction machine, the stator current overshoot is identified and analyzed in section 3. Proposed algorithms to limit the stator current and minimize speed drop are presented in sections 4 and 5, respectively. Simulation results verify the effectiveness of proposed techniques in section 6.

### 2. Principles of DTC-SVM and Loss

The block diagram of DTC-SVM with optimal efficiency control is shown in Fig.1. The reference value of the stator flux is generated from the optimal efficiency control block. The optimal efficiency control is adopted from [23]; the optimal flux is function of reference speed and torque. The torque reference is generated by the PI controller from the speed error term. The inverter's voltage commands are provided by the PI controllers that regulate the flux amplitude and torque. The reference voltage components are generated in an arbitrary reference frame, hereafter referred to as the stator flux-oriented frame. The x-axis of this reference frame is aligned with the maximum of

stator flux, and the y-axis component of the stator flux is zero.

In DTC drive with optimal efficiency mode of control, the reference flux must be changed in accordance with the changed in load torque. When a sudden change in load torque occurs, the flux cannot be

adjusted immediately, and it will be done with delay. During this transient time, the DTC drive is able to produce torque proportional to the instant stator flux and y-axis current component in the stator flux-oriented reference frame.

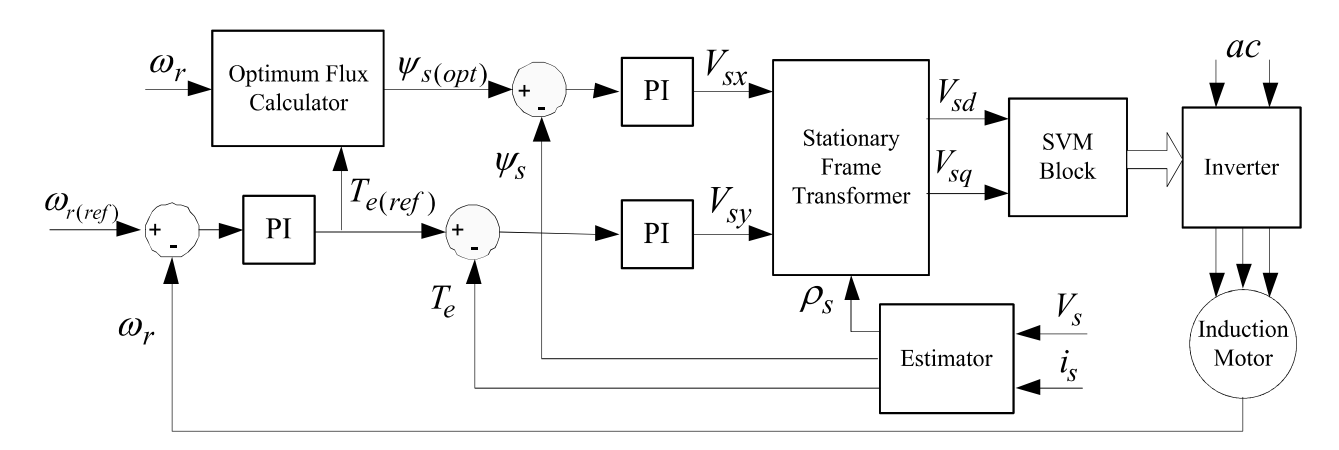


Fig. 1. Block diagram of DTC-SVM and loss minimization

## 3. Dynamic Model of Induction Motors

Using the stator flux-oriented frame (Fig. 2), the dynamic behavior of the induction machine is characterized by [24], [25], [26]:

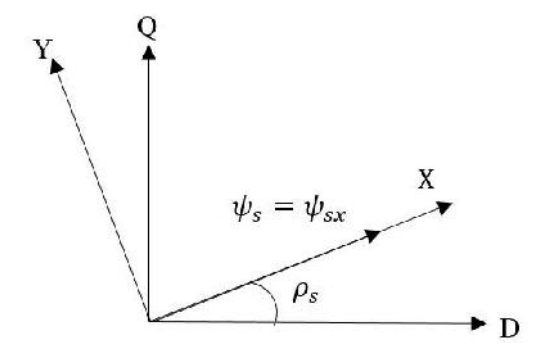


Fig. 2. The stationary reference frame and x-y reference frame fixed to the stator flux-linkage space phasor

$$V_{sx} = R_s i_{sx} + \frac{d\psi_s}{dt} \tag{1}$$

$$V_{sy} = R_s i_{sy} + \omega_{ms} \psi_s \tag{2}$$

$$V_{rx} = 0 = R_r i_{rx} + \frac{d\psi_{rx}}{dt} - (\omega_{ms} - \omega_r)\psi_{ry}$$
(3)

Downloaded from jiaeee.com on 2025-11-02

$$V_{ry} = 0 = R_r i_{ry} + \frac{d\psi_{ry}}{dt} - (\omega_{ms} - \omega_r)\psi_{rx}$$
 (4)

$$\psi_{S} = \psi_{SX} = L_{S}i_{SX} + L_{m}i_{rX} \tag{5}$$

$$\psi_{sv} = 0 = L_s i_{sv} + L_m i_{rv} \tag{6}$$

$$\psi_{rx} = L_m i_{sx} + L_r i_{rx} \tag{7}$$

$$\psi_{rv} = L_m i_{sv} + L_r i_{rv} \tag{8}$$

$$T_e = 1.5P\psi_{xx}i_{xy} \tag{9}$$

Where  $V_{sx}$ ,  $V_{sy}$  and  $V_{rx}$ ,  $V_{ry}$  represent stator and rotor voltage components respectively.  $i_{sx}$ ,  $i_{sy}$  and  $i_{rx}$ ,  $i_{ry}$  are stator and rotor current components respectively.  $\psi_{sx}$ ,  $\psi_{sy}$  and  $\psi_{rx}$ ,  $\psi_{ry}$  are stator and rotor flux components respectively.  $\psi_s$  is the value of stator flux.  $R_s$ ,  $R_r$  represent the stator and rotor resistance.  $L_s$ ,  $L_r$  and  $L_m$  are the self and mutual inductances.  $\omega_{sl}$  is the slip angular speed expressed in electrical radians,  $\omega_{ms}$  is the speed of stator flux-oriented frame, and  $\omega_r$  is the rotor angular speed expressed in electrical radians.  $T_e$  is the electrical torque and P is the number of pole-pairs

If the leakage inductance of stator and rotor are neglected then:  $L_{ls} = L_{lr} \cong 0$ ,  $L_s = L_r \cong L_m$ . According



fournal of Iranian Association of Electrical and Electronics Engineers - Vol.12- No.3- Winter 2015

to (5) and (7) results:  $\psi_{sx} \approx \psi_{rx}$ , and using (6) and (8) result:

$$\psi_{rv} \approx \psi_{sv} = 0 \tag{10}$$

$$i_{sv} \cong -i_{rv} \tag{11}$$

If the induction motor operates at constant flux condition,  $\psi_s = \psi_{sx} \cong cte$ , so:

$$V_{sx} = R_s i_{sx} \tag{12}$$

Substituting (10) in (3) gives:

$$i_{rx} \cong 0 \tag{13}$$

According to (5) and (13), one may have

$$\psi_S = \psi_{SX} \cong L_S i_{SX} \tag{14}$$

According to (12) and (14), a linear relation exists between  $V_{sx}$ ,  $i_{sx}$ ,  $\psi_{sx}$ . According to (2) and (9), a linear relation exists between  $V_{sy}$ ,  $i_{sy}$ ,  $T_e$  at the constant flux condition. Thus, with a constant flux, the stator current does not have any overshoot. However, an induction motor with optimal efficiency control has a variable stator flux. Therefore, the stator current overshoots from its permissible value. It will be proved in the next section.

### 3.1. X-Y Axis Equivalent Circuit

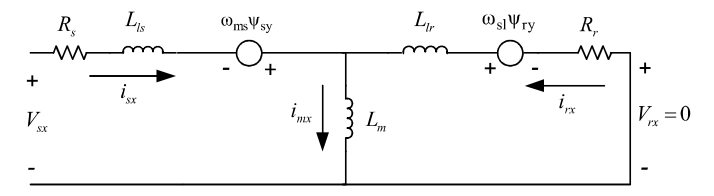
By using (1)-(4), equivalent circuit of the induction motor in stator flux-oriented frame is shown in Fig. 3, where  $i_{mx}$  and  $i_{my}$  are magnetizing current components.

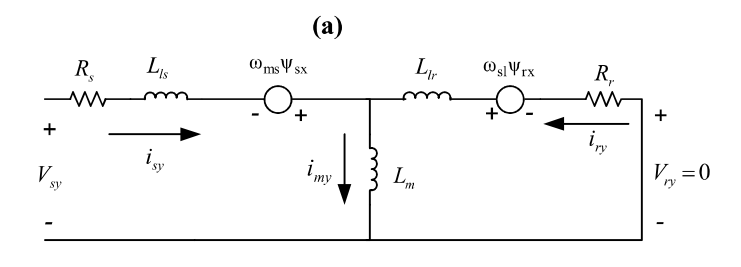
# 3.1.1. Analysis of X-axis Component of Stator Current $(i_{sx})$

According (6), the y-axis component of the stator flux is zero in stator flux-oriented frame. Therefore, the voltage source in the left part of x-axis equivalent circuit in Fig. 3-a,  $(\omega_{ms}\psi_{sy})$  is short circuit. If leakage inductances are neglected, according (10), the y-axis component of the rotor flux is zero too. So the voltage source in the right part of x -axis circuit in Fig. 3-a,  $(\omega_{sl}\psi_{ry})$  is short circuit. Therefore, the x-axis equivalent circuit simplifies as shown in Fig. 4.

The X-axis equivalent circuit is a resistance-inductor circuit, so if the voltage source  $V_{sx}$  changes suddenly, the current will overshoot. Besides according to Fig. 1,  $V_{sx}$  is the output of PI controller, where the flux error is the input of PI controller. Therefore, if the reference stator flux increases (for example at instant t=0+),

 $V_{sx}$  suddenly increases to the maximum available value. Thus, the x-axis component of stator current overshoots at t=0+, where the reference stator flux increases. The rate of this overshoot will be presented in next section.





(b)
Fig. 3. Equivalent circuit of an induction motor: (a) X-axis, (b) Y-axis

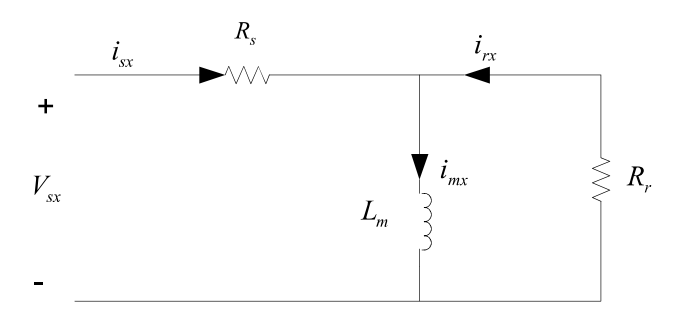


Fig. 4. Simplified x-axis equivalent circuit

## **3.1.2.** Analysis of y-axis component of stator current $(i_{sv})$

According to (11):

$$i_{mv} = i_{sv} + i_{rv} \stackrel{\sim}{=} 0 \tag{15}$$

Therefore,  $v_{my} = 0$  and the y-axis of equivalent circuit of Fig. 3-b, can be simplified as Fig. 5

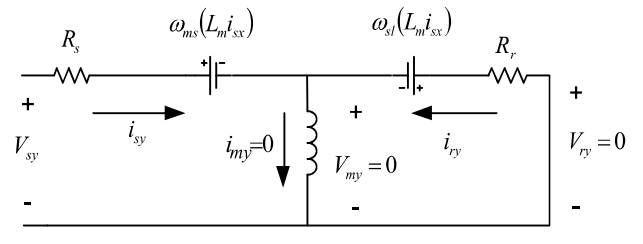


Fig. 5. Simplified y-axis equivalent circuit

According to Fig. 5, the relation between  $V_{sy}$  and  $i_{sy}$  can be written as:

$$V_{SV} = R_S i_{SV} + \omega_{mS} (L_m i_{SX}) = R_S i_{SV} + \omega_{mS} \psi_{SX}$$
 (16)

If the stator flux is at its nominal value, and the reference torque changes, then the reference  $V_{sy}$  suddenly increases to its maximum available value.  $i_{sy}$  reaches its nominal value and based on (9), the torque reaches its reference value. Therefore, the stator current does not have any overshoot and is limited to its nominal value.

If the stator flux is smaller than its nominal value, and the torque reference changes to nominal value, the  $V_{sy}$  reference suddenly increases to the maximum available value that is equal to its nominal value, Based on (16),  $i_{sy}$  exceeds its nominal value. Therefore, the stator current exceeds its nominal value. For example, suppose the nominal values of  $i_s$ ,  $i_{sx}$  and  $i_{sy}$  are 20, 11 and 17 amperes, respectively. Suppose the induction motor operates at light loads and, to optimize efficiency, the stator flux is set to 60% of its nominal value and  $i_{sx}$  is about 6.6 amperes. When the motor load changes to its nominal value, according to (9),  $i_{sy}$  reaches 28.5 amperes. Therefore, the stator current reaches 30 amperes, which is equal to 150% of its nominal value.

## 3.2. Stator Current Overshoot with Dynamic Flux

In order to find the stator current overshoot, it is assumed that the motor drive system works under an initial stator flux  $\psi_s(0)$  and a generate torque  $T_e$ , then the stator flux references changes to a new value  $\psi_{s(ref)}$ . Using the dynamic model of the induction motor, the initial transient value for  $i_s$  is obtained as follows (appendix A)

$$i_{s}(0^{+}) = \sqrt{i_{sx}^{2}(0) + i_{sy}^{2}(0)} = \sqrt{\left(\frac{\psi_{s}(0)}{L_{m}} + \frac{K_{p}\Delta\psi_{s}}{R_{r}}\right)^{2} + \left(\frac{T_{e(ref)}}{1.5P\psi_{s}(0)}\right)^{2}}$$
(17)

where  $i_s(0^+)$  is the initial overshoot of the stator current and Kp is the proportional gain of the PI flux controller.

For the motor drive system of Fig. 1 with parameters  $R_r = 0.35$   $L_m = 0.086$ ,  $K_p = 50$ ,  $K_i = 500$ , using (17), the current overshoot for three states with different values of initial flux  $\psi_S(0)$  is given in Table I. It is

Downloaded from jiaeee.com on 2025-11-02

assumed that, the stator flux  $\Psi_s$ , is changed from the initial value  $\psi_s(0)$  to new value,  $\psi_{s(ref)}$ . For example, in the third state, the drive works under 40 N.m torque,

the stator flux  $\psi_s$  has increased from 0.5 to 0.8 (Wb), and the stator current amplitude is 50 A.

Table. 1. Stator Current Overshoot value during change in flux

No.	$\psi_s(0)$	Ψs(ref)	$T_e$	Transient Stator Current Overshoot $i_s(0^+)$		
State1	0.0	0.8	0.0	114		
State2	0.8	0.5	10	33		
State3	0.5	0.8	40	50		

## 4. Proposed Current Limiting Algorithm

The DTC-SVM drive with torque controller using a conventional optimum flux calculator is shown in Fig. 1. The reference flux must be changed in accordance with the change in load. Therefore, the stator current amplitude exceeds its rated value, and the inverter's rated power must be increased. In the proposed strategy here, the reference flux is applied to SVM-DTC as a ramp instead of in step form. The proposed reference flux is shown in Fig. 6. It is noteworthy that, if one uses a steep slope, the current will exceed its rated value. Otherwise, if the slope is smooth, a long time is needed to achieve the flux reference. Therefore, there should be an optimum slope. In the following, an algorithm is developed to calculate the optimum slope.

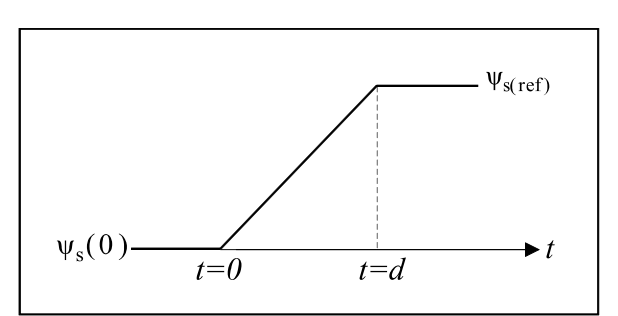


Fig. 6. The proposed reference flux.

According to Fig. 6, the new reference flux can be written as:

$$\psi_{S(ref)}(t) = \psi_{S}(0) + mtu(t) - m(t-d)u(t-d)$$
(18)

where, u(t) is the unit function, d is duration of ramp and m is the slope given by:

$$m = \frac{\psi_{S}(ref) - \psi_{S}(0)}{d} = \frac{\Delta \psi_{S}}{d}$$
 (19)

Laplace transform of (18), can be written as:



Journal of Iranian Association of Electrical and Electronics Engineers - Vol. 12- No. 3- Winter 201

$$\psi_{s(ref)}(s) = \frac{\psi_{s}(0)}{s} + \frac{m}{s^{2}}(1 - e^{-ds})$$
 (20)

 $V_{sx}$  can be obtained from PI controller of flux error as:

$$V_{sx}(s) = K_p(\psi_{s(ref)}(s) - \psi_s(s))$$

$$+\frac{K_i}{s}(\psi_{s(ref)}(s) - \psi_s(s)) \tag{21}$$

According to (21) and (A2)

$$\psi_{s}(s) = \frac{\psi_{s}(0)s + \psi_{s(ref)}(s)K_{p}s + \psi_{s(ref)}(s)K_{i}}{(s^{2} + sK_{p} + K_{i})}$$
(22)

$$\psi_{s}(s) = \frac{\psi_{s}(0)}{s} + \left(\frac{m}{s^{2}} - \frac{m}{s^{2} + sK_{p} + K_{i}}\right) \left(1 - e^{-ds}\right)$$

$$= \frac{\psi_{s}(0)}{s} + \left(\frac{m}{s^{2}} - \frac{k_{3}}{s + A} \frac{k_{4}}{s + B}\right) \left(1 - e^{-ds}\right)$$
(23)

Where:

$$A = -\left(\frac{K_p + \sqrt{K_p^2 - 4K_i}}{2}\right) \tag{24}$$

$$B = -\left(\frac{K_p - \sqrt{K_p^2 - 4K_i}}{2}\right)$$

$$k_3 = \frac{m}{B - A}, k_4 = \frac{m}{A - B} \tag{25}$$

From (23), the stator flux can be found:

$$\psi_{s}(t) = \psi_{s}(0) + (mt - k_{3}e^{-At} - k_{4}e^{-Bt})u(t) - \left(m(t-d) - k_{3}e^{-A(t-d)} - k_{4}e^{-B(t-d)}\right)u(t-d)$$
(26)

By substituting (26) in (A11), the  $i_{sx}$  for  $0 \le t \le d$  can be written as:

$$i_{sx}(t) = \frac{\psi_s(0)}{L_m} + \frac{m}{R_r} + \frac{mt}{L_m} - \left(\frac{k_3}{L_m} - \frac{Ak_3}{R_r}\right) e^{-At}$$
$$-\left(\frac{k_4}{L_m} - \frac{Bk_4}{B}\right) e^{-Bt}$$
(27)

Then, according to (27):

$$i_{sx}(0^{+}) = \frac{\psi_{s}(0)}{L_{m}} + \frac{m}{R_{r}} - \left(\frac{k_{3}}{L_{m}} - \frac{Ak_{3}}{R_{r}}\right) e^{-Ad}$$

$$-\left(\frac{k_{4}}{L_{m}} - \frac{Bk_{4}}{R_{r}}\right) = \frac{\psi_{s}(0)}{L_{m}}$$
(28)

Therefore,  $i_{sx}$  does not have any overshoot when the new reference flux is applied. According to (27), the maximum value of  $i_{sx}$  occurs at t=d:

$$i_{sx}(d) = \frac{\psi_{s(ref)}}{L_m} + \frac{m}{R_r} - \left(\frac{k_3}{L_m} - \frac{Ak_3}{R_r}\right) e^{-Ad} - \left(\frac{k_4}{L_m} - \frac{Bk_4}{R_r}\right) e^{-Bd}$$
(29)

By substituting (25) in (29):

$$i_{SX}(d) = \frac{\psi_{S(ref)}}{L_m} + \frac{m}{R_r} + P \tag{30}$$

where

$$P = \frac{m}{A - B} \left( \left( \frac{1}{L_m} - \frac{A}{R_r} \right) e^{-Ad} - \left( \frac{1}{L_m} - \frac{B}{R_r} \right) e^{-Bd} \right)$$
 (31)

According to (24), A is smaller than B. Therefore, P is negative and

$$i_{SX}(d) < \frac{\psi_{s(ref)}}{L_{m}} + \frac{m}{R_{r}}$$
(32)

On the other hand, the  $i_{sx}$  should not exceed the maximum permissible value. Therefore:

$$i_{sx(\text{max})} = \frac{\psi_{s(ref)}}{L_m} + \frac{m}{R_r}$$
(33)

and

$$m = R_r \left( i_{sx(\text{max})} - \frac{\psi_{s(ref)}}{L_m} \right)$$
 (34)

where:

$$i_{sx(\text{max})} = \sqrt{i_{inv(\text{max})}^2 - i_{sy}^2}$$
 (35)

where  $i_{inv(max)}$  is the maximum amplitude of permitted inverter current.

According to (9), (34) and (35):

$$m = R_r \left( \sqrt{i_{inv(\text{max})}^2 - \left( \frac{T_e}{1.5 P \psi_s} \right)^2} - \frac{\psi_{s(ref)}}{L_m} \right)$$
 (36)

The adequate ramp for flux reference can be determined by using  $R_r$ ,  $L_m$ ,  $T_e$ ,  $\Psi_{S}(ref)$ ,  $\Psi_{S}$  and  $i_{inn(max)}$  in (36).

The block diagram of proposed method is shown in Fig. 7.

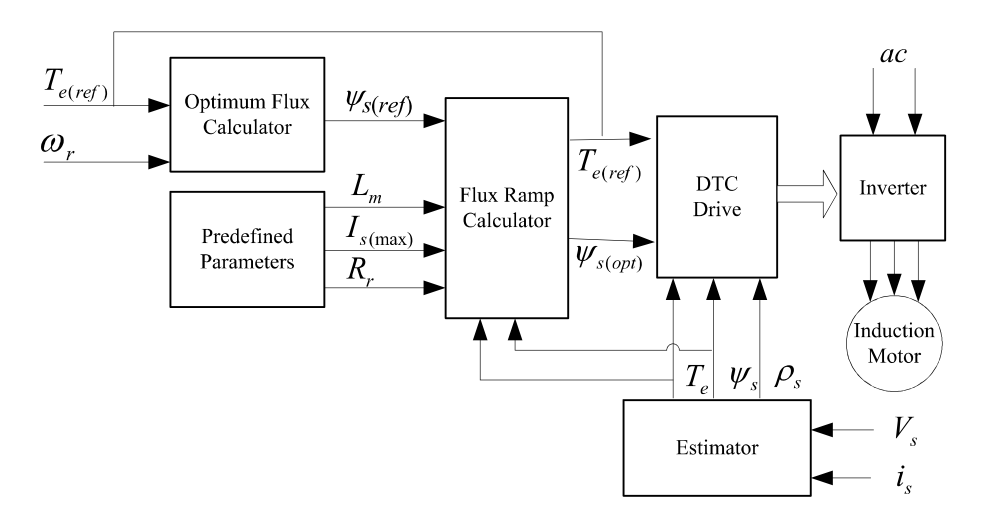


Fig. 7. Block diagram of proposed current limiting algorithm

## 5. Minimizing Drop in Speed

In a DTC-SVM drive, with a speed controller using the conventional optimum flux calculator in Fig. 1, when the induction motor drive operates at optimal efficiency, the flux level is reduced for small values of load torque. In this condition, a sudden increase in the load torque can lead to severe speed drop. In this section, an algorithm is proposed to minimize the speed drop in the DTC of an induction motor, when load torque suddenly increases. To do so, first the electric torque of the induction motor is formulated as a function of the rotor flux and maximum allowable inverter current. Then, the optimal flux, that minimizes the speed drop, is obtained. It will be used as a flux reference.

## 5.1. Torque Formulation of Induction Motor

The electromagnetic torque of induction motor in rotor flux-oriented frame can be calculated as [24]:

$$T_e = \frac{3PL_m}{2L_r} \psi_r i_{qs} \tag{37}$$

here  $L_r$  and  $L_m$  are respectively, rotor self and mutual inductances, P is the number of pole-pairs,

 $\psi_r$  is the value of rotor flux, and  $^{lqs}$  is the stator current component in q-axis. The rotor voltage, in rotor flux-oriented frame, can be expressed as:

$$0 = R_r \overline{i}_r + \frac{d\overline{\psi}_r}{dt} + j(\omega_{mr} - \omega_r)\overline{\psi}_r \tag{38}$$

Downloaded from jiaeee.com on 2025-11-02

Where  $\overline{\psi}_r$  and  $\overline{i}_r$  are the space phasor of rotor flux and current respectively in rotor flux-oriented frame, respectively,  $R_r$  represents the rotor resistance,  $\omega_r$  is

the rotor angular speed expressed in electrical radians, and  $\omega_{mr}$  is the speed of rotor flux-oriented frame. By using d-axis component of (38), the change in rotor flux can be expressed as:

$$\frac{d\psi_r}{dt} = -R_r i_{dr} \tag{39}$$

The space phasor of rotor flux can be calculated as:

$$\overline{\psi}_r = L_r \overline{i}_r + L_m \overline{i}_s \tag{40}$$

By using d-axis component of (40), the d-axis component of rotor current,  $i_{dr}$ , can be found as a function of  $\psi_r$  and d-axis component of stator current,

$$i_{dr} = \frac{\psi_r - L_m i_{ds}}{L_r} \tag{41}$$

Substituting (41) in (39), d-axis component of stator current can be calculated as a function of rotor flux:

$$i_{ds} = \frac{L_r}{R_r L_m} \frac{d\psi_r}{dt} + \frac{\psi_r}{L_m} \tag{42}$$

The maximum allowable inverter current,  $i_{inv(max)}$ , is distributed into the d-q axis current, such that during transients:

$$i_{qs} = \sqrt{i_{inv(max)}^2 - i_{ds}^2}$$
 (43)

Substituting (42) in (43), the q-axis component of the stator current can be calculated as a function of rotor flux:

$$i_{qs} = \sqrt{i_{inv(max)}^2 - (\frac{L_r}{R_r L_m} \frac{d\psi_r}{dt} + \frac{\psi_r}{L_m})^2}$$
 (44)

Substituting (44) in (37), the electromagnetic torque can be calculated as a function of rotor flux:



Journal of Iranian Association of Electrical and Electronics Engineers - Vol.12- No.3- Winter 2015

$$T_{e} = \frac{3PL_{m}}{L_{r}} \psi_{r} \sqrt{i_{inv(max)}^{2} - (\frac{L_{r}}{R_{r}L_{m}} \frac{d\psi_{r}}{dt} + \frac{\psi_{r}}{L_{m}})^{2}}$$
(45)

## 5.2. Analysis of Speed Drop

Let an induction machine operate in the steady state at light load, with reduced stator flux levels and optimum efficiency. A sudden load torque increase happens, at time instant zero, leading to the operation of the inverter at maximum allowed current value  $i_{inv(max)}$ . During transient time, the machine's speed drop can be defined as:

$$\Delta\omega = \frac{1}{J}(T_e - T_L)\Delta t \tag{46}$$

Where J is the total inertia of the drive, and  $T_e$  and  $T_L$  are the electrical and load torque respectively. Substituting (45) in (46), speed drop can be written as:

$$\Delta\omega = \frac{1}{J} \left[ \left( \frac{3PL_m}{L_r} \psi_r \right) \right]$$

$$\sqrt{i_{inv(max)}^2 - \left( \frac{L_r}{R_r L_m} \frac{d\psi_r}{dt} + \frac{\psi_r}{L_m} \right)^2} - T_L \right] \Delta t$$
(47)

The discrete form of (47), can be expressed as:

$$\Delta\omega = \frac{1}{J} \left[ \left( \frac{3PL_m}{L_r} \psi_r(n) \right) \right]$$

$$\sqrt{i_{inv(\text{max})}^2 - \left( \frac{L_r}{R_r L_m} \frac{\psi_r(n) - \psi_r(n-1)}{\Delta t} + \frac{\psi_r(n)}{L_m} \right)^2} \left( \frac{1}{2} \right)$$

$$- T_L \left[ \Delta t \right]$$

The optimal value of  $\psi_r(n)$  for minimizing  $\Delta\omega$  can be calculated as:

$$\frac{d\Delta\omega}{d\psi_r(n)} = 0\tag{49}$$

From (49),  $\psi_r(n)$  can be calculated as a function of  $\psi_r(n-1)$ .

$$\psi_r(n) = \frac{\psi_r(n-1)(6B+3D\Delta t) + \sqrt{E}}{8(C\Delta t^2 + D\Delta t + B)}$$
(50)

Where:

$$A = i_{inn(\max)}^2, B = \left(\frac{L_r}{R_r L_m}\right)^2, C = \left(\frac{1}{L_m}\right)^2, D = \frac{2L_r}{R_r L_m^2}$$
 (51)

$$E = \psi_r (n-1)(4B^2 + 4DB\Delta t + 9D^2 \Delta t^2 - 32CB\Delta t^2)$$

$$+8A\Delta t^2 (4C\Delta t^2 + 4D\Delta t + 4B)$$
(52)

If the rotor flux is equal to  $\psi_r(n)$  in (50), it is guaranteed that the produced torque will be the

maximum feasible torque, when the inverter current will not be more than the maximum allowable current. Therefore, the speed drop will be minimized. The stator flux is used as the reference frame in DTC-SVM drives, and its amplitude is regulated. Therefore, the  $\psi_s$ , is formulated as a function of the rotor flux  $\psi_r$ . To achieve this, the stator flux phasor is written as:

$$\overline{\psi}_{S} = L_{S}\overline{i}_{S} + L_{m}\overline{i}_{P} \tag{53}$$

Solving (40) and (53) with respect to rotor and stator currents, the rotor current phasor,  $\bar{i}_s$  is found as a function of  $\overline{\psi}_s$  and  $\overline{\psi}_r$ . Then substituting in (38), it is obtained:

$$\frac{d\overline{\psi}_r}{dt} = -\left[\frac{R_r}{\sigma L_r} + j(\omega_{mr} - \omega_r)\right]\overline{\psi}_r + \frac{R_r L_m}{\sigma L_s L_r}\overline{\psi}_s \tag{54}$$

where  $\sigma = 1 - \frac{L_m^2}{L_s L_r}$  is the leakage coefficient. The d-axis component of (54), is expressed as:

$$\frac{d\psi_r}{dt} = \frac{-R_r}{\sigma L_r} \psi_r + \frac{R_r L_m}{\sigma L_s L_r} \psi_{ds}$$
 (55)

Where  $\psi_{ds}$  and  $\psi_{qs}$  are the stator flux components in rotor flux frame, respectively. The torque can be expressed as [24]:

$$T = 3P \frac{L_m}{\sigma L_s L_r} \overline{\psi}_r \times \overline{\psi}_s \tag{56}$$

Equation (56), can be expressed in the rotor flux reference frame as:

$$T = 3P \frac{L_m}{\sigma L_s L_r} \psi_r \times \psi_{qs} \tag{57}$$

By using (55) and (57),  $\psi_{ds}$  and  $\psi_{qs}$  can be obtained

as a function of  $\psi_r$  and  $T_e$ . The discrete form of these

equations can be expressed as:

$$\psi_{ds}(n) = \frac{L_s}{L_m} (\psi_r(n) + \frac{\sigma L_r}{R_r} \frac{\psi_r(n) - \psi_r(n-1)}{\Delta t})$$
 (58)

$$\psi_{qs}(n) = \frac{\sigma L_r L_s}{P L_m} \frac{T_e(n)}{\psi_r(n)}$$
(59)

So the magnitude of stator flux,  $\psi_s$  is:

$$\psi_{s}(n) = \sqrt{\psi_{ds}^{2}(n) + \psi_{as}^{2}(n)}$$
 (60)

Finally, to obtain the proper stator flux and torque references to minimize the speed drop, the algorithm depicted in Fig. 8 can be used in every step.

[ Downloaded from jiaeee.com on 2025-11-02

Accordingly, first by using the value of  $\psi_r(n-1)$  and (50)-(52),  $\psi_r(n)$ , and then by using (58)-(60), the corresponding value of  $\psi_{s(ref.s)}$  is obtained. Further,

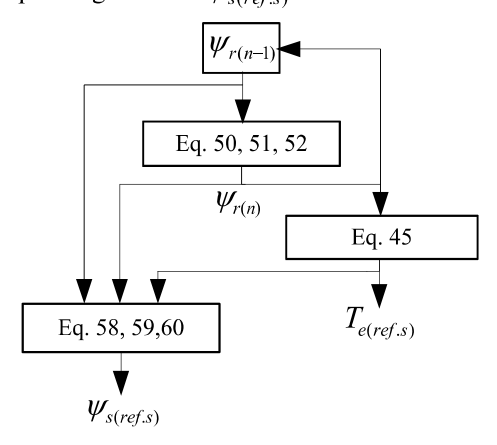


Fig. 8. An algorithm to minimize speed drop

using (45), and considering the maximum permitted current,  $T_{e(ref.s)}$  is obtained and applied to the system. Therefore, the maximum torque is generated and minimum speed drop is achieved, while the inverter current does not exceed its maximum permitted value. Fig. 9 shows the block diagram of proposed algorithm for minimizing the speed drop, when sudden load torque increase, in optimal efficiency control operation. The dynamic state detector, using the speed error, distinguishes the status of load torque changing. If  $\omega_r < 0.95\omega_{r(ref)}$ , it means that the load torque has suddenly increased. Then, speed drop minimization algorithm is activated,  $\psi_{s(ref)}$  and  $T_{e(ref)}$  are calculated and applied to DTC. Otherwise  $\omega_r > 0.95\omega_{r(ref)}$ ; the drive is almost working in steady-state condition with nominal or light load torque. Then  $\psi_{s(ref)}$  is calculated using optimum flux algorithm and  $T_{e(ref)}$  is the same as the input torque reference. In the following, these references value are applied to DTC by signal selector.

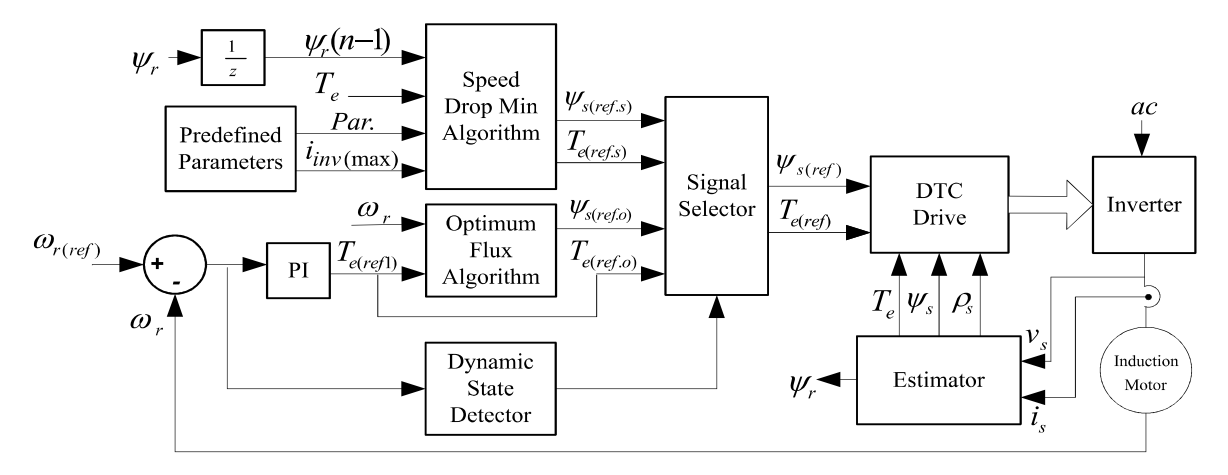


Fig. 9. Block diagram of proposed speed drop minimization algorithm

### 6. Simulation Results

The optimal efficiency DTC-SVM drives are simulated using MATLAB/SIMULINK, and the results of conventional and improved methods are compared. The motor parameters are given in table II, [27].

To validate the effectiveness of the optimal efficiency control block, the DTC drive has been tested with different load torques in two cases: first with the nominal flux, and then with the optimal flux. The results of efficiency are shown in Table III, and it is seen that by using the optimal efficiency block, the efficiency has improved especially in low load torque.

i abie.	۷.	induction	Motor	Parameters	ì
	_				

Parameter	Value
Rated Power	9 kW
Rated Current (rms/amplitude)	20/28.3 A
Number of Pole Pairs	4
Stator Resistance	$0.399~\Omega$
Stator Leakage Inductance	2.7 mH
Magnetizing Inductance	86.6 mH
Rotor Resistance	$0.3538~\Omega$
Rotor Leakage Inductance	3.8 mH
Inertia ( J )	$0.03 \text{ kg.m}^2$

Journal of Iranian Association of Electrical and Electronics Engineers - Vol.12- No.3- Winter 2015

Table. 3. DTC drive efficiency with different load torques

Torque	Efficiency in	Efficiency in
(N.m)	nominal flux	optimal flux
	(percent %)	(percent %)
5	44	65
20	61	71
40	76	76

## 6.1. DTC-SVM Drive with Torque Controller

The block diagram of the DTC-SVM drive with torque controller, Fig. 7 is simulated. In this mode of operations, the reference torque profile is predefined, and directly applied to DTC drive, and it is supposed that, the torque load is  $T_l = 0.22\omega_m$ . The reference flux is generated from the optimum flux calculator block and applied to DTC, simultaneously. In the conventional method, the reference flux is directly applied to the DTC drive. In the proposed method, the modified reference flux is calculated from the flux ramp calculator block and applied to the DTC drive.

First, the DTC-SVM drive is simulated without limiting the stator current. Initially,  $T_{ref} = 0$  and the reference torque is stepped up to 10(N.m) at t=0.2(sec), and then stepped up again to 40(N.m) at t=0.4(sec). Fig. 10-a, 10-f shows the reference torque, motor torque, motor speed, stator flux, and stator current amplitude. As seen at the starting point, the stator current amplitude reaches 120(A). When the reference torque increases, the stator current overshoots to approximately 50(A). The inverter must be designed to deliver these high currents.

Alternatively, the DTC-SVM drive with the proposed flux ramp calculator is considered. The reference flux is applied in form of a ramp. The flux ramp is calculated by Eq. (36) to limit the maximum amplitude of permitted inverter current,  $i_{inv(max)}$ . For example, when the reference torque is stepped to 40(N.m) at t=0.4(sec), according to Eq.(36) and table II, m=3.1(wb/sec) for  $i_{inv(max)}=30(A)$ . Fig. 11-a, 11-f shows the dynamic operation of motor states in this method As seen in Fig. 11-f, at starting point and when the reference torque increases, the stator current amplitude is limited to 30(A); equal to the maximum inverter's current.

### **6.2. DTC-SVM Drive with Speed Controller**

The block diagram of the DTC-SVM drive with a speed controller, shown in Fig. 9, is simulated. In this mode of operations, the reference speed is applied to the drive. The motor initially operates in the steady state under  $T_L = 10 \text{ (N.m)}$  and  $\omega_{ref} = 10 \text{ (rad/s)}$ . Load torque is then increased to 40 (N.m) at t=0.4(sec).

First, the DTC-SVM drive, with conventional optimum flux algorithm, is simulated. In this case the

optimal value of stator flux, for loss minimization, is applied to DTC at all times and dynamic state detector is bypassed. Fig. 12-a to 12-g show speed, electrical torque, torque reference, d and q axis components of stator current in stator-flux reference frame, stator flux, and efficiency of motor.

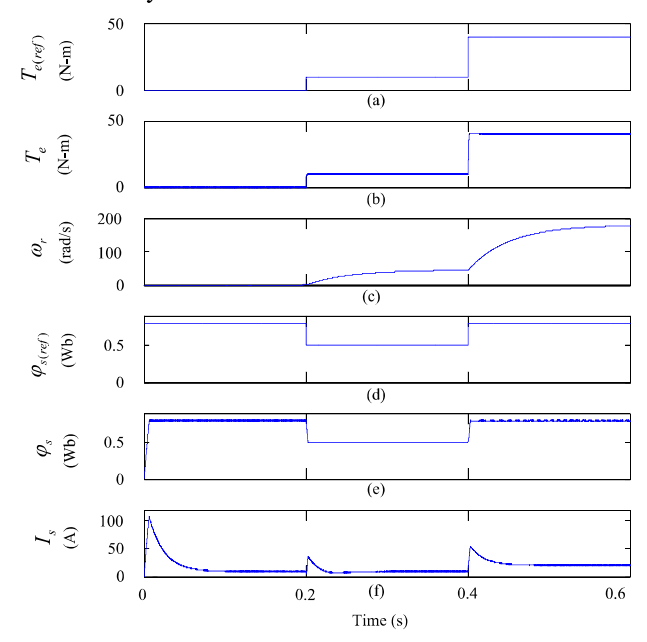


Fig. 10. DTC-SVM drive with torque controller using a conventional optimum flux calculator, (a) Torque reference, (b) Electrical torque, (c) Speed, (d) Stator flux reference, (e) Stator flux, and (f) Stator current

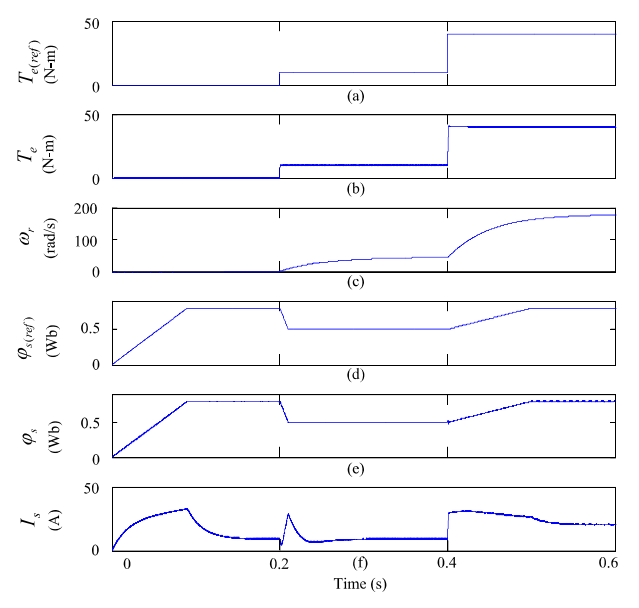


Fig. 11. DTC-SVM drive with torque controller using the proposed flux ramp calculator (a) Torque reference, (b) Electrical torque, (c) Speed, (d) Stator flux reference, (e) Stator flux, and (f) Stator current

The load torque is initially small and equal to 10 (N.m), so the reduced optimum flux, is computed by the block of optimum flux algorithm, and applied to the

[Downloaded from jiaeee.com on 2025-11-02

system as the flux reference. At t=0.4 (sec), when the load torque suddenly increases, the motor flux is still at a reduced value, and starts to increase slowly and with delay. As a result, motor's ability to generate torque is reduced, and the speed drops 4.5 (rad/s), as shown in Fig. 12-a. Also it is seen that in the steady state efficiency for a light load torque of 10 (N.m) is 0.68, and for high load 40 (N.m) is 0.72.

Alternatively, the DTC-SVM drive with the proposed algorithm to minimize the speed drop is simulated. In this case the optimal stator flux for loss minimization is initially applied in steady state. After increasing the load torque, the dynamic state detector diagnosis new statues, and the optimal stator flux that is computed by speed drop minimization algorithm, will be applied to DTC. Fig. 13-a, 13-g shows the dynamic operation of motor states in this method. In this case, the speed reduction after the sudden load increase is 1.2 (rad/sec), which is smaller than the conventional method. However, the loss-minimizing algorithm via flux reduction is considered here too. Therefore, the steady state efficiency for a light load torque of 10 (N.m) is 0.68, and for high load 40 (N.m) is 0.72, and it is the same as previous test.

#### 7. Conclusion

The induction motor operates with a reduced flux level at light loads, when the conventional DTC-SVM with optimal efficiency control is applied. The sudden increase in load torque causes the reference flux to increase, and the stator current overshoots. When the load torque increases suddenly, speed will drop significantly, since the flux-level has initially been reduced. This phenomenon has been analyzed here, and a suitable method to limit the stator current is proposed for DTC-SVM with a toque controller. The reference flux is applied to DTC in a ramp form with an optimum slope. This significantly lowers the inverter's rating compared to the conventional methods. Moreover, to improve the dynamic performance while preventing the speed drop, an algorithm has been proposed for the DTC-SVM with a speed controller. Using this algorithm, the inverter current will keep the maximum allowable value, the maximum torque is produced, and the speed drop in response to the sudden load change is minimized. The proposed algorithms are validated using numerical simulations.

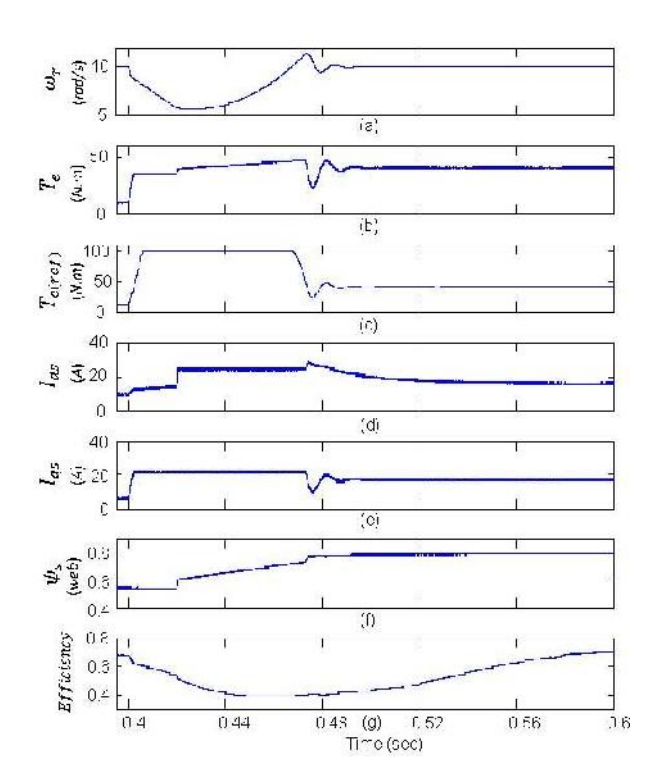


Fig. 12. DTC-SVM drive with the speed controller using conventional optimum flux algorithm. (a) Speed, (b) Electrical torque, (c) Torque reference, (d-e) d and q axis components of stator current in stator flux reference frame, (f) Stator flux, and (g) Efficiency of motor.

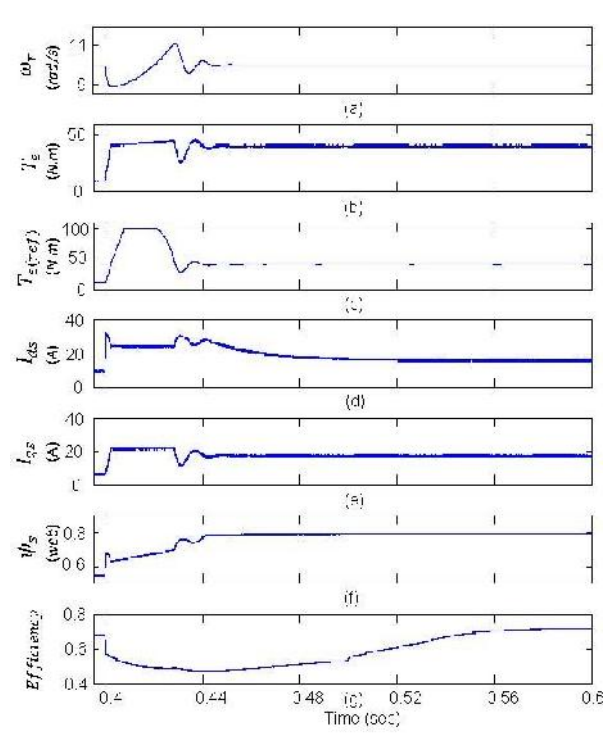


Fig. 13. DTC-SVM drive with the speed controller using speed drop minimization algorithm (a)Speed, (b) Electrical torque, (c) Torque reference, (d-e) d and q axis components of stator current in stator flux reference frame, (f) Stator flux, and (g) Efficiency of motor.



Journal of Iranian Association of Electrical and Electronics Engineers - Vol. 12- No.3- Winter 2015

## Acknowledgment

The authors would like to thank S. Abhinav and S.A Hashemi for their help in this paper.

### References

- [1] N.R. Idris, C.L. Toh and M.E. Elbuluk, "A new torque and flux controller for direct torque control of induction machines," IEEE Trans. Ind. Appl., vol. 42, no. 6, pp. 1358-1366, Nov./Dec. 2006.
- [2] S. Vaez-Zadeh, E Jalali, "Combined vector control and direct torque control method for high performance induction motor drives," Energy conversion and management, vol. 48, no. 12, pp. 3095-3101, Dec. 2007.
- [3] SP.Yalla, P. Pugazhendiran, K.Sarmila Har, "Synthesized Direct Torque Control for high-power induction motor drive," in Intelligent 2013 7th International Conference on Systems and Control (ISCO), 2013, pp. 79 83.
- [4] T.G. Habetler, F. Profumo, "Direct torque control of induction machines using space vector modulation," IEEE Trans. Ind. Electron., vol. 28, no. 5, pp. 1045-1053, 1992.
- [5] T. Nathenas, G. Adamidis, "A new approach for SVPWM of a three-level inverter induction motor fedneutral point balancing algorithm," Simulation Modelling Practice and Theory, vol. 29, pp. 1-17, 2012
- [6] W. Wang, M. Cheng, W. Hua, "A low-cost SVM-DTC strategy of induction machine drives using single current sensor," in International Conference on Electrical Machines and Systems (ICEMS), China 2011, pp. 1-7.
- [7] J. Gholinezhad, R. Noroozian, "Application of Cascaded H-Bridge multilevel inverter in DTC-SVM based induction motor drive," in 3rdPower Electronics and Drive Systems Technology (PEDSTC), 2012, pp. 127-132
- [8] J. Jeyashanthi, V. Hemamaheswari, G.L. Thilagam, G. Loganayaki, "A novel approach for a multirate 3 level carrier SVM of DTC based IM drive," in International Conference on Recent Advancements in Electrical, Electronics and Control Engineering (ICONRAEeCE), 2011, pp. 78-81.
- [9] J.F. Stumper, A. Dotlinger, R. Kennel, "Loss Minimization of Induction Machines in Dynamic Operation," Energy Conversion, IEEE Transactions on, vol. 20, no. 99, pp. 1 – 10, 2013.
- [10] J.R. Dominguez, C. Mora-Soto, S. Ortega-Cisneros, J.J.R. Panduro, A.G. Loukianov, "Copper and core loss minimization for induction motors using high order sliding mode", IEEE Transactions on Industrial Electronics, vol. 59, no. 7, pp. 2877-2889, 2012.
- [11] M.N. Uddin, S.W. Nam, "Adaptive back stepping based online loss minimization control of an IM drive," in: IEEE Power Engineering Society General Meeting, Canada, 2007, pp. 1-9.
- [12] D. Biswas, K. Mukherjee, N.C. Kar, "A novel approach towards electrical loss minimization in vector controlled induction machine drive for EV/HEV," in: IEEE Transportation Electrification Conference and Expo (ITEC), Canada, 2012, pp. 1-5.

- [13] J.R. Dominguez, C. Mora-Soto, S. Ortega-Cisneros, J.J.R. Panduro, A.G. Loukianov, "Copper and core loss minimization for induction motors using high order sliding mode," IEEE Transactions on Industrial Electronics, vol. 59, no. 7, pp. 2877-2889, 2012.
- [14] M.N. Uddin, S.W. Nam, "New online loss minimization based control of an induction motor drive," IEEE Trans. Power Electron., vol. 23, no. 2, pp.926-933, 2008.
- [15] D. Kim, K. Hirota, "Vector control for loss minimization of induction motor using GA-PSO," Applied Soft Computing, vol. 8, no. 4, pp. 1692-1702, 2008.
- [16] S. Lim, K. Nam, "Loss minimization control scheme for induction motor," IEE Proceedings - Electric Power Applications, vol. 151, no. 4, pp. 385 – 397, July 2004.
- [17] AM. Bazzi, PT. Krein, "Review of methods for realtime loss minimization in induction machines," Industry Applications, IEEE Transactions on, vol. 46, no. 6, pp. 2319 – 2328, 2010.
- [18] G.S. Kim, "Control of induction motors for both high dynamic performance and high power efficiency," Industrial Electronics, IEEE Transactions on, vol. 39, no. 4, pp. 323 – 333, Aug 1992.
- [19] I.T. Wallace, D.W. Novotny, "Increasing the dynamic torque per ampere capability in saturated induction machines," IEEE Trans. Ind. Appl., vol.30, no.1, pp. 146-153.1994.
- [20] S.N. Vukosavic, E. Levi, "A method for transient torque response improvement in optimum efficiency induction motor drives," IEEE Trans. Energy conversion, vol. 18, no. 4, pp. 484 – 493, 2003.
- [21] Casadei, D.; Serra, G.; Stefani, A.; Tani, A. "DTC Drives for Wide Speed Range Applications Using a Robust Flux-Weakening Algorithm," Industrial Electronics, IEEE Transactions on, vol. 54, no. 5, pp. 2451 – 2461, 2007.
- [22] Jidin, A., Idris, N.R.N.; Yatim, A.H.M.; Sutikno, T. "An Optimized Switching Strategy for Quick Dynamic Torque Control in DTC-Hysteresis-Based Induction Machines," Industrial Electronics, IEEE Transactions on, vol. 58, NO. 8, pp. 3391 – 3400, 2011.
- [23] M.H. Ershadi, M. Moallem and M.Ebrahimi, "Loss-minimization scheme in modified DTC-SVM for induction motors with torque ripple mitigation," Journal of Applied Sciences, vol. 10, no. 19, pp. 2269-2275, 2010.
- [24] P. Vas, Sensorless vector and direct torque control, Oxford University, 1998.
- [25] Y. Kumsuwan, H. Toliyat, "Modified direct torque control method for induction motor drives based on amplitude and angle control of stator flux," Electric Power Systems Research, vol. 78, no. 10, pp. 1712-1718, 2008.
- [26] GH. R. Arab Markadeh, M. Sadogh, "Direct Torque and Power Factor Control of Induction Motor with Input-Output Linearization using Matrix Converter," Journal of Iranian Association of Electrical and Electronics Engineers, vol. 8, no. 1, pp. 31-39, 2011.
- [27] M.H. Ershadi, "Torque ripple minimization and dynamic performance improvement in optimal efficiency DTC control of induction motors," Ph.D. dissertation, Isfahan University of Technology, 2012.
- [28] J. Soltani et al, "Direct Torque and flux control of Reluctance motor by SVM Bi-Level Inverter using

Slipping Controller "Journal of Iranian Association of Electrical and Electronics Engineers, Vol. 3,No.1, 2006.

[29] H. Moayedirad et al, "Induction Machine Drive Performance Improvement in low and high Speed Range with flux Compensation", Journal of Iranian Association of Electrical and Electronics Engineers, Vol. 9.No.2, 2012.

## **Appendix A. Stator Current Overshoot** with Dynamic Flux

In this appendix, the stator current overshoot is found using the dynamic model of induction motor. According to (1), if the stator resistance is neglected,

 $V_{sx}$  can be obtained as:

$$\psi_s(n) = \sqrt{\psi_{ds}^2(n) + \psi_{qs}^2(n)}$$
 (A 1)

Laplace transform of (A1), can be written as:

$$V_{SX}(s) = s \psi_S(s) - \psi_S(0)$$
 (A2)

On the other hand,  $V_{sx}$  can also be obtained from the PI controller of flux error as:

$$V_{sx}(s) = K_p \left( \frac{\psi_{s(ref)}}{s} - \psi_s(s) \right) + \frac{K_i}{s} \left( \frac{\psi_{s(ref)}}{s} - \psi_s(s) \right)$$
(A 2)

From (A2) and (A3), Laplace form of the stator flux can be written as:

$$\psi_{s}(s) = \frac{\psi_{s}(0)s^{2} + \psi_{s(ref)}K_{p}s + \psi_{s(ref)}K_{i}}{s(s^{2} + sK_{p} + K_{i})}$$

$$= \frac{\psi_{s(ref)}}{s} + \frac{k_{1}}{s + A} + \frac{k_{2}}{s + B}$$
(A 3)

Where:

$$A = -\left(\frac{K_p + \sqrt{K_p^2 - 4K_i}}{2}\right)$$

$$B = -\left(\frac{K_p - \sqrt{K_p^2 - 4K_i}}{2}\right)$$

$$k_1 = \frac{A(\psi_s(ref) - \psi_s(0))}{B - A}$$

$$k_2 = \frac{B(\psi_s(ref) - \psi_s(0))}{4 - B}$$
(A 4)

From (A4), the stator flux can be found:

$$\psi_s(t) = \psi_{s(ref)} + k_1 e^{-At} + k_2 e^{-Bt}$$
 (A 5)

Using x-axis component of rotor voltage [24], one may conclude:

$$0 = L_m \frac{di_{sx}}{dt} - \omega_{sl} L_m i_{sy} + R_r i_{rx} + L_r \frac{di_{rx}}{dt} - \omega_{sl} L_r i_{ry}$$
(A 6)

Components of the rotor current can be written as:

$$i_{rx} = \frac{\varphi_{sx} - L_s i_{sx}}{L_m}, i_{ry} = -\frac{L_s}{L_m} i_{sy}$$
 (A 7)

Moreover, from (A7) and (A8):

$$0 = \frac{R_r}{L_m} (\varphi_{sx} - L_s i_{sx}) + \frac{L_r}{L_m} \frac{d\varphi_{sx}}{dt} + k \frac{di_{sx}}{dt} - (\omega_{ms} - \omega_r)(ki_{sy})$$
(A 8)

Where:

$$k = \left(\frac{L_m^2 - L_s L_r}{L_m}\right) \tag{A 9}$$

If the leakage inductances stator are neglected, k=0 and (A9), is simplified to:

$$i_{SX} = \frac{\psi_S}{L_m} + \frac{1}{R_r} \frac{d\psi_S}{dt}$$
(A 10)

Substituting (A6) in (A11) leads to:

$$i_{sx} = \frac{\psi_s}{L_m} + \left(\frac{k_1}{L_m} - \frac{Ak_1}{R_r}\right) e^{-At}$$

$$+ \left(\frac{k_2}{L_m} - \frac{Bk_2}{R_r}\right) e^{-Bt}$$
(A 11)

Thus, the initial value of the x-axis stator current is:

$$i_{sx}(0^{+}) = \frac{\psi_{s}}{L_{m}} + \frac{k_{1}}{L_{m}} - \frac{Ak_{1}}{R_{r}} + \frac{k_{2}}{L_{m}} - \frac{Bk_{2}}{R_{r}}$$
(A 12)

Substituting (A5) in (A13) leads to:

$$i_{SX}(0^+) = \frac{\psi_S(0)}{L_m} + \frac{K_p(\Delta\psi_S)}{R_r}$$
 (A 13)

When the reference torque is constant, the initial and final values for  $i_{SV}$  can be calculated from (9):

$$i_{SY}(0) = \frac{T_{e(ref)}}{1.5P\psi_{s}(0)}$$
 (A 14)

The initial transient value for  $i_s$  can be calculated as:

$$i_{s}(0^{+}) = \sqrt{i_{sx}^{2}(0) + i_{sy}^{2}(0)}$$

$$= \sqrt{\left(\frac{\psi_{s}(0)}{L_{m}} + \frac{K_{p}\Delta\psi_{s}}{R_{r}}\right)^{2} + \left(\frac{T_{e(ref)}}{1.5P\psi_{s}(0)}\right)^{2}}$$
(A 15)





